

On the role of hydrophobic Si-based protective coatings in limiting mortar deterioration

G. Cappelletti¹ · P. Fermo¹ · F. Pino¹ · E. Pargoletti¹ · E. Pecchioni² · F. Fratini³ · S. A. Ruffolo⁴ · M. F. La Russa⁴

Received: 10 April 2015 / Accepted: 24 June 2015 / Published online: 9 July 2015
© Springer-Verlag Berlin Heidelberg 2015

Abstract In order to avoid both natural and artificial stone decay, mainly due to the interaction with atmospheric pollutants (both gases such as NO_x and SO₂ and particulate matter), polymeric materials have been widely studied as protective coatings enable to limit the penetration of fluids into the bulk material. In the current work, an air hardening calcic lime mortar (ALM) and a natural hydraulic lime mortar (HLM) were used as substrates, and commercially available Si-based resins (Alpha[®]SI30 and Silres[®]BS16) were adopted as protective agents to give hydrophobicity features to the artificial stones. Surface properties of coatings and their performance as hydrophobic agents were studied using different techniques such as contact angle measurements, capillary absorption test, mercury intrusion porosimetry, surface free energy, colorimetric measurements and water vapour permeability tests. Finally, some exposure tests to UV radiation and to real polluted atmospheric environments (a city centre and an urban background site) were carried out during a wintertime period (when the concentrations of the main atmospheric

pollutants are higher) in order to study the durability of the coating systems applied. The effectiveness of the two commercial resins in reducing salt formation (sulphate and nitrate), induced by the interaction of the mortars with the atmospheric pollutants, was demonstrated in the case of the HLM mortar.

Keywords Mortars · Hydrophobic coatings · Water capillarity · Transpirability · UV ageing · External exposure

Introduction

Nowadays, the conservation and restoration of cultural heritage are an important issue difficult to be completely solved, especially in the case of historical buildings and monuments, which are seriously affected by environmental conditions and atmospheric pollution (Doehne and Price 2010; Ghedini et al. 2011; Tidblad et al. 2012).

The study of some materials constituting the historical buildings, such as mortars or marbles, is of interest because these materials maintain and transmit to us, not only the aspect of an artefact, but also information on the ancient technologies used to realize the artefact itself. This contributes to improve the knowledge of our past and our history, and also provides useful data for the conservation of cultural heritage (Pecchioni et al. 2008).

In particular, the present study is focused on mortars which are materials used in architecture with very different functions: as bedding mortars in the masonries, as filling of the wall nucleus, as rendering of walls, support for mural paintings, up to material to join decorations, etc. (Moropoulou et al. 2000; Elsen 2006; Faria et al. 2008)

In some historical buildings, mortars have been used to realize ornamental elements, ashlar or, sometimes, the complete façade. This artificial stone could be either a mortar

Responsible editor: Philippe Garrigues

✉ G. Cappelletti
giuseppe.cappelletti@unimi.it

¹ Dipartimento di Chimica, Università degli Studi di Milano, Via Golgi 19, 20133 Milano, Italy

² Dipartimento di Scienza della Terra, Università degli Studi di Firenze, Via G. La Pira 4, 50121 Firenze, Italy

³ CNR-Istituto per la Conservazione e la Valorizzazione dei Beni Culturali, Via Madonna del Piano 10, 50019 Sesto Fiorentino, Firenze, Italy

⁴ Dipartimento di Biologia, Ecologia e Scienze della Terra (DiBEST), Università della Calabria, Via Pietro Bucci, Cubo 12 B, 87036 Arcavacata di Rende, Cosenza, Italy

“worked” directly in situ or an ornamental element prepared in mould (Pecchioni et al. 2005).

However, like any other materials, mortars undergo a deterioration process, and this is closely related to the adaptation of the material structure to the surrounding environment. The extent of the degradation depends on both internal factors (compositional characteristics and fabrication techniques) and external ones (the combined action of physical, chemical and biological factors) (Pecchioni et al. 2008). Among the external causes, atmospheric pollution is mainly responsible for the deterioration of historical monuments placed in urban areas, where the concentrations of the pollutants (both gases such as NO_x and SO_2 and particulate matter) reach the highest values (Zappia et al. 1998; Brimblecombe 2003; Watt et al. 2009; Tidblad et al. 2012). NO_x and SO_2 are emitted mainly by combustion processes (traffic, heating plants, industrial emissions) and it is well known that in the atmosphere, can be converted into the corresponding acids or can act as gaseous precursors leading to the formation of secondary aerosols (such as ammonium nitrate and ammonium sulphate). Both acidic species and particulate matter interact with the material surfaces inducing deterioration processes. In particular, the main reaction that takes place is the conversion of calcium carbonate into gypsum (Brimblecombe 2003; Watt et al. 2009; Belfiore et al. 2013; La Russa et al. 2013; Fermo et al. 2014b; Ruffolo et al. 2015). Moreover, the majority of the degradation phenomena occurs in the presence of water and in particular because of its penetration into the material bulk; so, the deterioration is favoured in mortars that allow an easier water absorption (Pecchioni et al. 2008; Ruffolo et al. 2014).

The best way to avoid mortar decay is the protection by surface treatment with polymers, due to their ability to form a protective layer on the monument surface as well as to control the transport of different fluids from the surface to the bulk. Traditionally, polymeric resins, acrylic and vinyl polymers, organosilicone compounds, fluorinated film forming agents have been applied to stone monuments as protective hydrophobic films against stone deterioration (Alessandrini et al. 2000; Tsakalof et al. 2007).

Besides the reduction of water absorption, many criteria must be met for the successful application of a specific coating, such as good adhesion, mechanical and physical durability, transparency, no colour and/or reflectance changes. The characteristics of the coatings applied have been widely studied, as well as the specific interactions between the material surface and the hydrophobic layer (Fermo et al. 2014a).

In this work, an air hardening calcic lime mortar (ALM) and a natural hydraulic lime mortar (HLM) were used as substrate. Commercially available Si-based resins (Alpha[®]SI30 by Sikkens and Silres[®]BS16 by WackerChemie AG) were used as protective polymers to give hydrophobicity features to the substrate, in order to improve their resistance against atmospheric pollutants. Surface properties of coatings and

their performance as protective agents were studied using different techniques such as contact angle measurements, capillary absorption test, mercury intrusion porosimetry, colorimetric measurements and water vapour permeability tests. Finally, the durability and the effect of ageing caused by the prolonged exposure to real environmental conditions will be discussed.

Materials and methods

Mortar preparation

Two typologies of mortars have been manufactured, one utilizing an air hardening calcic lime and the other with a natural hydraulic lime. A total of 10 samples for each type have been prepared with dimension $5 \times 5 \times 5$ cm (Fig. 1).

The air hardening calcic lime mortar (ALM, Fig. 1) has been realized with an aggregate constituted by a quartz-feldspar sand (CTS-restoration products-Florence: grain size 0.3–0.5 mm) and, as binder, a lime putty matured 7 years [“Calce Viva” 90-S-PL (according to UNI EN 459-1:2010)(UNI EN 2010)] produced by Adriatica Legnami in Fasano (Apulia) utilizing wood as combustible, commercialized and guaranteed by “La Banca della calce” (Bologna), according to a binder/aggregate ratio of 1/3 (Table 1). Water has not been added because utilizing the lime putty only some drops of lime wash are sufficient for a good workability of the mix.

The natural hydraulic lime mortar (HLM, Fig. 1) has been realized with the same type of sand (quartz-feldspar sand by CTS-restoration products-Florence: grain size 0.3–0.5 mm) and as binder, a natural hydraulic lime [NHL 3.5 (according to UNI EN 459-1:2010)(UNI EN 2010)] produced by “Calce Raffinata” in Savignano sul Panaro (Emilia) according to a binder/aggregate ratio of 1/3 (Table 1). Deionized water has been added according to a binder/water ratio of 0.66, sufficient to allow a good kneading.

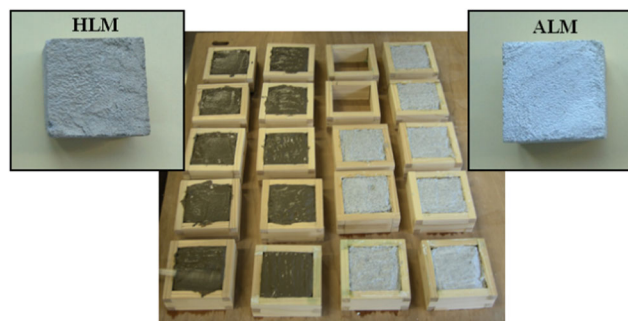


Fig. 1 Representative photographs of wet and dry HLM/ALM mortars

Table 1 Composition of mortar substrates

Component	Natural hydraulic lime mortar (HLM)	Air hardening calcic lime mortar (ALM)
Aggregate	Silicatic sand (0.3 mm<d<0.5 mm)	Silicatic sand (0.3 mm<d<0.5 mm)
Binder	Natural hydraulic lime NHL 3.5	Lime putty matured for 7 years
Binder/aggregate Ratio	1/3	1/3
Water	Demineralized	–
Binder/water ratio	0.66	–

Hydrophobic coatings

Samples have been treated with different commercial water repellent protective agents:

- Alpha®SI30 (Sikkens) is declared as an oligomeric polysiloxane by the producer; it is colourless, waterproof and indicated to be used on materials such as plasters and natural stones. In previous works of some of the co-authors of this paper (Fermo et al. 2014a; Cappelletti et al. 2015), this resin has been finely characterized, and it was found to be composed by a mixture of a trimethoxysilane, where R could be a quite long chain (i.e. iso-octyl) and a poly-dimethyl-siloxane (PDMS). The resin was applied as it is without any dilution.
- Silres®BS16 (WackerChemie AG), a solution of potassium methyl silicate, develops its water-repellent properties by reaction with atmospheric carbon dioxide. The active substance formed from the silicone masonry water repellent is polymethylsilicic acid. SILRES®BS16 is supplied as a concentrate and was diluted with water (1:10), under vigorous stirring, before use.

The application of coatings on all the stone faces has been carried out by using brush in a homogeneous manner, in order to reproduce everyday working conditions. All the silane-coated mortars were dried for 24 h in an oven at constant temperature (50 °C).

Sample characterization

Powders obtained from each typology were analysed with a PANalytical diffractometer X’PertPRO with radiation CuKα (λ=1.545 Å), operating at 40 kV, 30 mA, investigated range 2θ=3–70°, equipped with X’ Celerator multirevelator and software PANalytical High Score for data acquisition and interpretation of the mineralogical composition.

Optical microscopy in transmitted light was performed on thin section (30 microns thickness). A polarized light microscope (ZEISS Axio Scope.A1) equipped with a camera (resolution 5 megapixel) was used in order to investigate the microstructural characteristics of the mortars (Pecchioni et al. 2006; Fratini et al. 2008).

Static contact angle measurements of water on bare and coated mortars were performed on a Krüss Easy instrument. A drop of 3 µL was produced and gently placed on the surface; the drop profile was extrapolated using an appropriate fitting function. Measurements were repeated several times to obtain a statistically relevant population (30 measurements each sample), since substrates were really variables even in near spots.

Colorimetric measurements (CIELab) were performed to verify the global colour modification ($\Delta E^* = \sqrt{\Delta L^{*2} + \Delta a^{*2} + \Delta b^{*2}}$) of the protective films after both the deposition of the protective coatings and accelerated UV/ambient exposure, where L^* , a^* and b^* are the lightness (0 for black–100 for white), the red–green component (positive for red and negative for green) and the yellow–blue component (positive for yellow and negative for blue), respectively. The three chromatic coordinates were calculated starting from diffuse reflectance spectra acquired in the UV–Vis spectral range from 800 to 300 nm (WI halogen lamp). The analyses were performed by Shimadzu UV-Visible Spectrophotometer equipped with the ISR-2600 0-degree/8-degree incidence integrating sphere. According to the literature, $\Delta E^* < 5$ was considered as corresponding to a not significant variation (Mahy et al. 1994; La Russa et al. 2012) over ten repeated readings for each sample.

The surface free energy (SFE) and the relative polar and disperse components were obtained by using the Owens–Wendt–Rabel–Kaelble (OWRK) method (Cappelletti et al. 2013). Contact angle measurements can be related to SFE of solids via Young’s equation (Young 1805):

$$\gamma_s - \gamma_{sl} = \gamma_{lv} \cos\theta$$

where θ is the measured contact angle, γ_s is the surface free energy (SFE) of the solid in the case of small or negligible spreading pressure π_e , γ_{sl} and γ_{lv} are the surface tensions at solid–liquid and liquid–vapour interface, respectively. This equilibrium is the basis for the calculation of the surface tension/surface energy components, and some models such as the Owens–Wendt–Rabel–Kaelble method (OWRK) (Owens and Wendt 1969; Kaelble 1970) distinguish a polar and a disperse fraction of the surface energy. The surface energy was calculated by exploiting the contact angle values

determined for water, ethylene glycol, diethylene glycol, glycerol and diiodomethane (Cappelletti et al. 2013).

The porosity was evaluated by means of the following methods: water saturation method (WSM) and mercury intrusion porosimetry (MIP). WSM is based on the determination of the open pore volume V_{op} (cm^3) which corresponds to the volume of water absorbed by the samples, according to the procedure reported in the European protocol (UNI EN 2001). The dried mortars (at 60 °C for 24 h) were placed in appropriate vessels and slowly covered with deionized water until they were totally immersed with about 2 cm of water above them. After 8 h, the samples were weighted, and the measurements were repeated until the difference in weight between two subsequent measurements at 24-h intervals was less than 1 % of the amount of water absorbed. Porosity and pore size distributions were also determined by MIP, through a Micromeritics Autopore IV with a maximum pressure of 400 MPa, according to the procedure reported in a previous work of some of the co-authors of this paper (Ruffolo et al. 2014). Measurements were performed on samples with the same weight (1.5 g) to standardize testing and minimize errors. This technique allowed to determine pore sizes ranging from 0.003 to 40 μm .

Capillary water absorption measurements were performed on bare and coated materials by the gravimetric sorption technique, minutely described in the Italian protocol Norma UNI 10859 “Cultural Heritage–Natural and artificial stones–determination of water absorption by capillarity”(NORMA UNI 2000). Each sample was dried in an oven at 60 °C for 7 days, put in a drier for 2 days and weighted. Then, all samples were placed on a multilayer of filter paper (thickness, 1 cm) saturated with deionized water in different closed vessels. The sample was extracted after fixed time intervals; after removing the water drops with a wet cloth, it was weighted again to determine the amount of water absorbed by capillary forces. Every test was performed at room temperature (25 ± 2 °C). As stated in the protocol, if the increase in relative weight at a distance of 24 h is below 1 %, the test is over. In some cases, after 8 days, the absorption curves of treated samples did not reach a plateau (no water saturation is reached). If the final condition could not be satisfied, tests were to be terminated after 8 days.

In order to evaluate the water vapour permeability of the film applied at the surface of the mortars, the methodology described in the European Standard EN 15803 (conservation of cultural property–test methods–determination of water vapour permeability δp , (UNI EN 2009)) was used.

Ageing and ambient exposure tests

The stability of the hydrophobic coatings (Alpha@SI30 and Silres@BS16) has been evaluated through accelerated ageing

tests under UV irradiation (500 W, 215–365 nm) for fixed time (40 h).

Further, with the aim to evaluate the protective action of the applied coatings, the substrates (bare stones and treated by both Si-based resins) were exposed in parallel in two typical urban environments placed in Milan and characterized by different conditions as concerns the impact of the main atmospheric pollutants (Gulotta et al. 2013; Fermo et al. 2014b). The first one is placed in the Milan University Campus (Fig. 2a), an area quite far from the city centre, that is considered representative of a typical urban background, while the second one is placed in Via Senato (Fig. 2b), that is in the city centre, close to one of the monitoring stations of the regional agency for the environmental protection (ARPA Lombardia), a site which is representative of a typical urban polluted environment (in the case of the site placed in Via Senato, it was possible to perform the field tests only for the commercial resin Alpha@SI30, which should be explained later on). In both sites, samples were not directly affected by rain runoff. The exposure tests were carried out for 110 days during winter (25 November 2013 to 15 March 2014). After the exposure, the concentration of NO_3^- and SO_4^{2-} on the treated and untreated samples was determined by ionic chromatography (IC). The samples were prepared according to a procedure reported elsewhere (Cappelletti et al. 2015). IC analyses were performed using an ICS-1000 instrument (Dionex-Thermo). The measurements were carried out by means of an Ion Pac AS14A (Dionex) column using 8 mM Na_2CO_3 /1 mM NaHCO_3 as eluent at 1 mL min^{-1} flow rate and, for the detection, a conductivity system equipped with an ASRS-ULTRA suppression mode (Dionex). The concentration of each ion was calculated using a calibration curve plotted by injecting working standard solutions obtained by dilution of stock solutions of 0.5, 1, 3, 5, 10 ppm. Analyses were run in triplicate, and the standard deviation was less than 5 %.

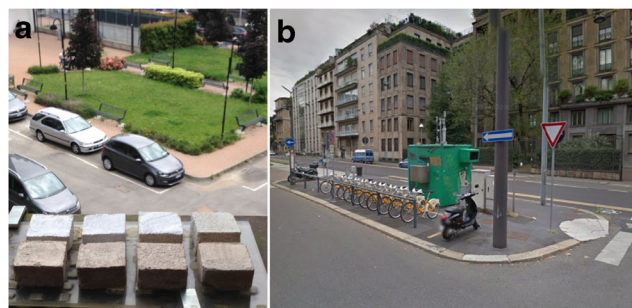


Fig. 2 Exposure sites: **a** Milan University Campus and **b** via Senato (city centre). The samples in the case **a** were placed on a covered balcony while in the case **b**, they were put inside a plastic two sides opened box, which was located on the roof of the monitoring station

Results and discussion

Mineralogical and petrographic features of the analysed mortars

The mineralogical analyses (XRD) have shown a sand composed by quartz (SiO_2), feldspars [$\text{W}(\text{ZO}_2)_4$], micas [$\text{W}_2(\text{X}, \text{Y})_{4-6} \text{Z}_8 \text{O}_{20}(\text{OH})_4$], chlorites [$(\text{Mg}, \text{Fe}, \text{Al})_{12}(\text{Si}, \text{Al})_8 \text{O}_{20}(\text{OH})_{16}$], lizardite [$\text{Mg}_6 \text{Si}_4 \text{O}_{10}(\text{OH})_8$] and pyroxenes [$\text{W}^{\text{VIII}}(\text{X}, \text{Y})_{1+p} \text{VI}(\text{Z}_2^{\text{IV}} \text{O}_6)$] (Carobbi 1971); thus, the resulting air hardening calcic mortar (ALM) has a composition of calcite and portlandite for the paste, and quartz, feldspars, chlorite, micas and lizardite for aggregates, while the hydraulic mortar (HLM) shows the same composition of ALM without the presence of portlandite.

The petrographic analyses in thin section have shown, for the air hardening calcic lime mortar (ALM, Fig. 3a, b), a binder with microsparitic texture and interference colour corresponding to first-order grey. Such characteristic confirms the only partial carbonation, as evidenced by XRD analysis that indicates the presence of portlandite. Indeed, it is well known that carbonation (which determines the hardening of the mortar) develops very slowly (in the course of months or years) as a function of the conditions of exposure to CO_2 and moisture, but also in function of the type of lime and composition of the

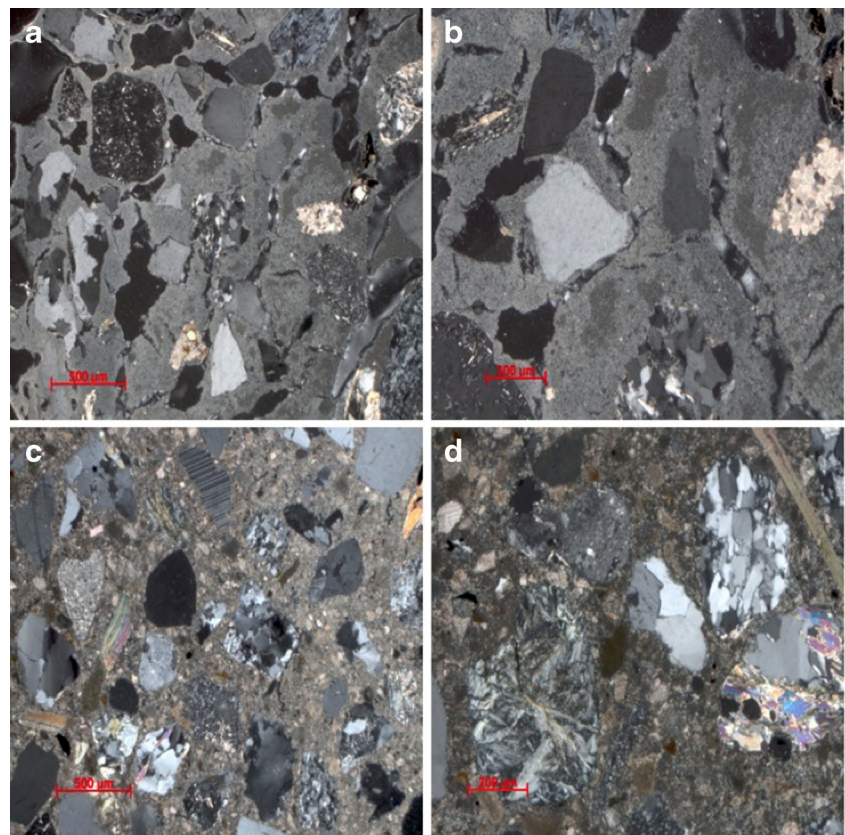
mortar (Pecchioni et al. 2008). The transition from hydroxide to carbonate occurs through the following phases:

1. Solubilisation of CO_2 in the water of the mix;
2. Dissolution of $\text{Ca}(\text{OH})_2$;
3. Evaporation of water;
4. Formation of carbonates for nucleation in the liquid phase;
5. Formation of carbonates for nucleation at the interface $\text{Ca}(\text{OH})_2/\text{H}_2\text{O}$.

The aggregate is well distributed in the mix and characterized by a unimodal grain size distribution (300–500 μm). It is constituted mainly by quartz and feldspar grains with sub-angular shape and by a lower amount of pyroxenes, micas and rock fragments (quartzite, sandstone, micaschists and serpentinite). The porosity is high and mostly with elongated shape.

Concerning the hydraulic lime mortar (HLM, Fig. 3c, d), a binder with microsparitic texture, brown in colour, rich in small underburnt lime fragments, is present. The aggregate is well distributed in the mix with unimodal grain size (300–500 μm) and a composition similar to that of the air hardening lime mortar. The porosity is high with both elongated and spherical pores (Pecchioni et al. 2014).

Fig. 3 Petrographic images in thin section of the ALM (a, b) and the HLM (c, d)



Surface properties of bare and coated mortars

It is well known that the application of Si-based resins allows to obtain hydrophobic protective coatings in the case of cultural heritage buildings and monuments (Kapridaki and Maravelaki-Kalaitzaki 2013; Fermo et al. 2014a).

Experimental static contact angle (SCA) measurements with water have been determined to evaluate the wettability features of the bare mortars; both the substrates (ALM and HLM) show a hydrophilic character ($\theta < 90^\circ$, Table 2, 2nd column). Notwithstanding the complete and almost immediate absorption of water drops, the evaluation of the contact angles has been performed by using the first frames taken by the video registration of deposition procedure. Both the substrates were produced with the same coarse aggregate ($0.3 \text{ mm} < d < 0.5 \text{ mm}$, see Table 1) demonstrating an intrinsic variability in their surface features; thus, the standard deviation of the contact angles is quite large, but this is statistically representing the variability of the sample. Hydraulic mortar (HLM) was more homogeneous and mechanically resistant (Jackson and Marra 2006; Belfiore et al. 2015); the SCA assessments on this kind of substrate were absolutely less problematic.

After the treatment with both the water-repellent agents (Alpha[®]SI30 and Silres[®]BS16), a successful hydrophobization of the substrates occurs ($\theta > 100^\circ$, Table 2, 2nd column). Similar results are reported in the recent literature: by depositing several commercial siloxane/silane resins on marbles and limestones (Zielecka and Bujnowska 2006; Karatasios et al. 2009; Manoudis et al. 2009a, b; Fermo et al. 2014a; Cappelletti et al. 2015), hydrophobic coatings are obtained, characterized by a maximum contact angle higher than 100° . Between the two resins, Alpha[®]SI30 gives the best results, especially onto the hydraulic mortar. This could be due to the presence of the adequate microporosity (see in the following) on the bare hydraulic mortar. It is generally well known that hydraulic features are given from the presence of silicates/aluminates in the starting material, which cause a different reactivity of the quicklime. This is of course reflected in a change of porosity as well. Alternatively, the better performance could be caused by the different interaction with resin in the presence of silicates (Fermo et al. 2014a).

Table 2 Static contact angles (θ) and colorimetric variation (ΔE^*) for bare and coated mortars

Sample	$\theta/^\circ$	ΔE^*
HLM	70±10	–
HLM_SI30	137±7	1.2±0.8
HLM_BS16	125±6	1.9±0.7
ALM	65±10	–
ALM_SI30	116±8	1.3±0.9
ALM_BS16	110±8	2.2±0.9

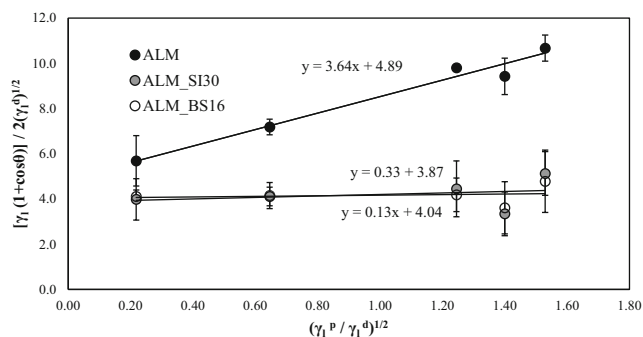


Fig. 4 OWKR elaboration for bare (ALM) and coated (ALM_SI30 and ALM_BS16) air hardening calcic lime mortars

Moreover, both the protective coatings were found to be transparent ($\Delta E^* < 5$, Table 2, third column); no colour variations are appreciable at human eye after the application of the hydrophobic layers.

Regarding the SFE results, Fig. 4 shows, as a representative samples, the linear trends of the data relative to both bare and coated (with the two different resins, Silres[®]BS16 and Alpha[®]SI30) air hardening calcic lime mortars (ALMs). The corresponding extrapolated results in terms of total SFE and polar (from the slope) components are reported in Table 3 (2nd and 3rd columns, respectively). Of course, it was not possible to obtain accurate values (high standard deviations) because of the intrinsic variability of the materials, both in the case of bare or coated ones, as stated previously. Anyway, interesting results were obtained: the decrease of the total surface energy values and particularly the polar part (lower than 1.0 mN/m) after the treatments is in agreement with the contact angle values obtained, confirming the hydrophobic features of the treated surfaces.

Water capillary absorption and vapour permeability

As it is reported by many studies in the literature, the prevention of water rising by capillary absorption plays a pivotal role in the conservation of historical buildings. This phenomenon is one of the main responsible in mortar degradation, since water freezing–melting cycles cause cracks and the transport of salts leads to formation of crusts.

Table 3 SFE values by Owens, Wendt, Rabel and Kaelble (OWRK) method

Sample	SFE $\gamma/\text{mN m}^{-1}$	Polar component $\gamma_p/\text{mN m}^{-1}$
HLM	33±10	15±5
HLM_SI30	<10	<1
HLM_BS16	<10	<1
ALM	37±7	13±3
ALM_SI30	15±6	<1
ALM_BS16	16±4	<1

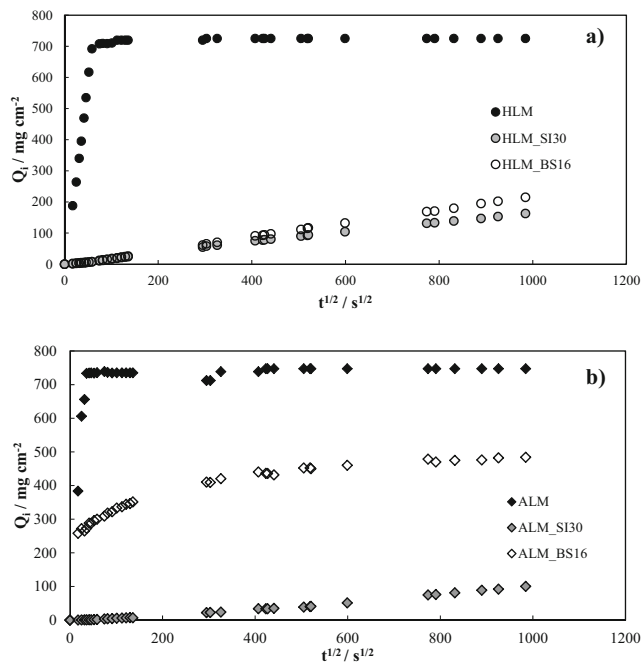


Fig. 5 Capillary absorption curves for **a** bare and coated hydraulic (HLM) and **b** air hardening calcic lime (ALM) mortars

The amount of water absorbed per unit area over time ($Q_i/\text{mg cm}^{-2}$) was plotted with respect to the square rooted time ($\text{s}^{1/2}$) for all the adopted mortars, both bare and Si-coated (Fig. 5). Besides, from the graphs, some parameters, typical of the present analyses, including the capillary absorption (CA) coefficient (that roughly represents the slope of the first 30 min of the absorption curve) and the capillarity index (IC, which is the ratio between integrated Q_i/\sqrt{t} areas and the corresponding area of the rectangle considering the same final time of the water absorption curve) were calculated and reported in Table 4. Particularly, the capillarity indices give information about the resistance to capillary rise when prolonged contact with water occurs.

An ideal protective coating should completely eliminate water absorption by capillary. For the untreated mortars, high amount of water was absorbed especially in the first hour for both the mortars (around $700 \text{ mg cm}^{-2} \text{ h}^{-1}$). When the pure resins were deposited on the mortar surface, a dramatic decrease in the capillary rise parameters (Table 4 and Fig. 5) for all of the treated samples occurs: the final Q_i collapses, the CA reduces of about two order of magnitude and the IC is halved, confirming the hydrophobic performances of both resins.

Anyway, Alpha®SI30 shows the best results while Silres®BS16 is less effective, especially in the case of ALM mortar.

However, alongside a complete block of water capillary rise, the water vapour transmission rate through the mortars must not be drastically reduced after the coating treatments, assuring the proper vapour regime inside the materials (Manoudis et al. 2009b). Thus, the impermeability of the mortar protective coating to water vapour could lead to material decay and polymer swelling. The reduction of vapour permeability caused by the coatings can be considered negligible up to 50 % as reported in the recent literature (Rodrigues and Grossi 2007). Thus, water vapour permeability tests were evaluated: Fig. 6 shows the cumulative mass change per unit area ($|\Delta m| = m_i - m_0$, where m_i and m_0 is the mass of the test assembly, respectively, at time t_i and t_0 , in kg) for each set of successive weighing of the specimens versus time for the determination of the steady-state water vapour diffusion flow through the tested materials. Both resins, applied on both mortars, show a good behaviour (Fig. 6a, b) with respect to water vapour permeability, leading to a small decrease (about 20–30 %) in material transpiration. This is fully in accordance with what is reported in the literature for highly hydrophobic silane- and silicone-derived coatings which maintain a high degree of permeability to water vapour (Kapridaki and Maravelaki-Kalaitzaki 2013), allowing stones to breath and at the same time reducing deterioration phenomenon, caused by external agents such as atmospheric pollution, as it will be shown later in the text.

The values of porosity, performed on treated and bare samples, assessed by means of water saturation method (WSM) and mercury intrusion porosimetry (MIP) are reported in Table 5. In the case of WSM, the data reveal a slight decrease in porosity after the hydrophobic treatments, both on ALM and in HLM samples. Instead, the results obtained by MIP do not show significant differences regarding the total open porosity percentage. Then, in order to better understand the porous structure of the mortars and its variations induced by the treatments, pore size distributions have been also reported in Fig. 7. HLM and ALM samples show quite different behaviour, since HLM mortar has a distribution that can be assumed as bimodal (at 0.35 and $\sim 10 \mu\text{m}$), while ALM mortar shows a trimodal distribution (at 0.15, 0.4 and $\sim 30 \mu\text{m}$). Moreover, ALM has smaller pores ($< 1 \mu\text{m}$) than HLM mortar. After the treatments, significant changes are shown for ALM

Table 4 Water capillary absorption parameters

	HLM	HLM_SI30	HLM_BS16	ALM	ALM_SI30	ALM_BS16
$Q_i/\text{mg cm}^{-2}$	725	139	180	747	81	475
$CA/\text{mg cm}^{-2} \text{ s}^{1/2}$	11.45	0.12	0.21	17.24	0.12	6.63
IC	0.96	0.53	0.50	0.97	0.43	0.87

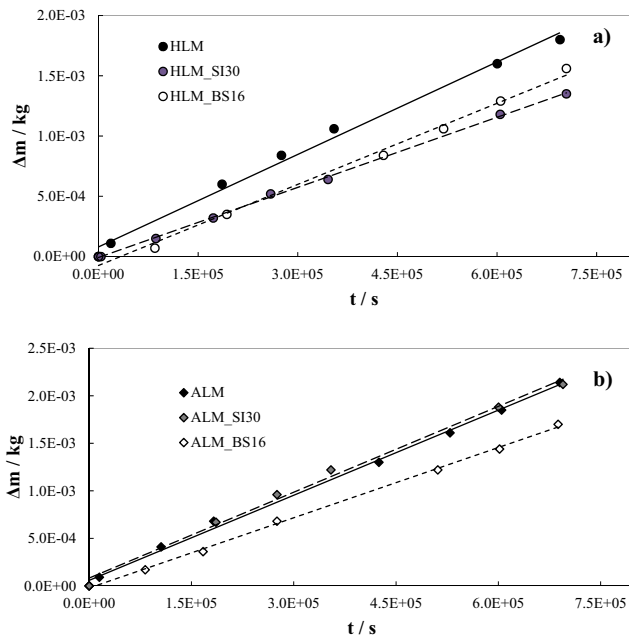


Fig. 6 Water vapour permeability plots in terms of variation of cumulative mass for bare and coated **a** hydraulic (HLM) and **b** air hardening calcic lime (ALM) mortars

mortar, since a shift of two peaks toward smaller size has been observed, due to a thin cladding of the pores; when this happens, the material is more prone to decay.

UV and ambient exposure

In order to evaluate the effect of atmospheric pollution on cultural heritage, field exposure tests are generally carried out (Manoudis et al. 2009b; Tidblad et al. 2012; Cappelletti et al. 2015). The aim of these tests is to assess the effectiveness of the protective coatings applied on the surfaces in the prevention, or at least reduction, of stone deterioration, i.e. mainly the sulphation that brings to the loss of material. Thus, some exposure tests have been performed at Milan University Campus and at the centre of the city (Fig. 2) on both not treated and coated mortars, and the salts (SO_4^{2-} and NO_3^-) concentration has been monitored. In a previous study (Cappelletti et al. 2015), the same approach has been

Table 5 Total open porosity values by water saturation (WS) and mercury (MIP) intrusion methods

	TOP _{WSM} (%)	TOP _{MIP} (%)
HLM	27±3	25±2
HLM_SI30	22±2	24±2
HLM_BS16	23±3	23±2
ALM	31±5	26±2
ALM_SI30	22±3	27±2
ALM_BS16	24±3	23±2

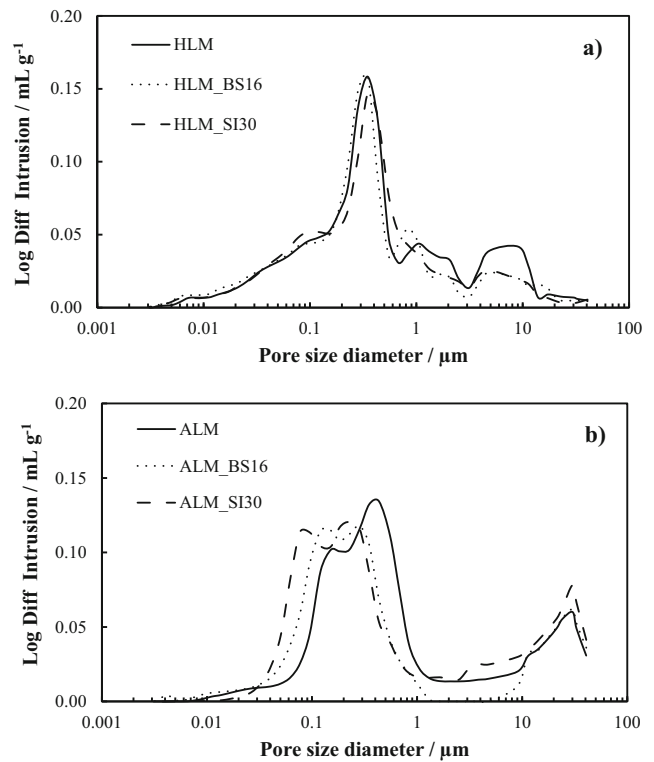


Fig. 7 Pore size distribution diagrams of bare and treated **a** hydraulic (HLM) and **b** air hardening calcic lime (ALM) mortars, obtained from mercury intrusion porosimetry

successfully followed to test the coating performances for the protection of some marbles.

As shown in Fig. 8 for both ALM and HLM, after about 4 months of exposure during winter 2013–2014, salts formation has been evidenced. Actually, the blank reference samples (not exposed) show significantly lower nitrate and sulphate concentrations. After the exposure, a different behaviour has been evidenced for the two mortars: in the case of HLM mortar, the application of both Silres®BS16 and Alpha®SI30 has allowed to reduce the formation of both salts, while in the case of ALM, the hydrophobic resins basically showed no protective effect against sulphate formation.

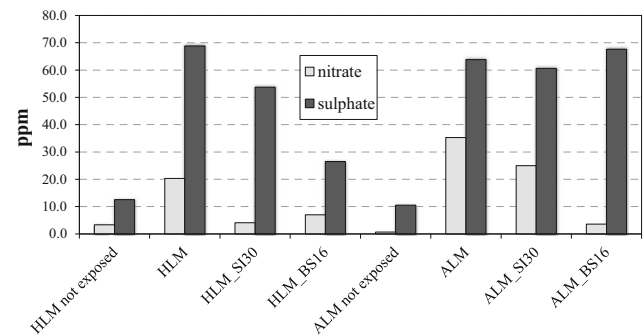


Fig. 8 Soluble salts concentration on the pure and treated adopted mortars, before and after exposure for 110 days during winter (25 November 2013 to 15 March 2014)

Table 6 Sulphate concentration after exposure tests

	SO ₄ ²⁻ /ppm	
	City Centre	Unimi Campus
HLM	1050	70
HLM_SI30	800	55
% reduction	24	21

The different physico-chemical properties of the two mortars, such as the chemical composition (Fig. 3), the crystalline phases and the porosity (Table 5, Fig. 7), seem to strictly affect the final performances. Particularly, ALM is less carbonated as demonstrated by the presence of portlandite (confirmed by XRD pattern, not shown); this feature is typical for example of ancient Roman mortars, as reported in the recent literature (Brandon et al. 2014). The lower carbonation determines both high specific surface and porosity of the sample (Table 5, WSM data). Since ALM is characterized by presence of pores with smaller dimension (see Fig. 7b), probably the resin cannot enter leading to a lower protection of the material, i.e. higher sulphation processes (Fig. 8). Looking at Fig. 8, it is evident how both resins are effective against nitrate formation, also in the case of ALM. This could be due to the fact that the reaction between Ca(OH)₂ (portlandite) and sulphuric acid, leading to the formation of stable products (gypsum), is more favourable with respect to the reaction between portlandite and nitric acid. However, the addition of a protective layer does not block the progressive sulphation of the material, while it reduces nitrate presence. Furthermore, at the same conditions, a material with smaller pores is more favourable to decay by salts than a material with larger pores.

Comparing the results obtained in the two exposure sites (Table 6), i.e. the University Campus and the Via Senato (in the city centre), it is evident how in the city centre, where pollutant concentrations present maximum values, a higher sulphate concentration has been determined for HLM mortar both not treated and coated with Alpha®SI30 (data for ALM are not reported since, as discussed before, the resins are not effective in this case). It is also worth noting that for both

exposure sites, the percentage efficiency of Alpha®SI30 in reducing sulphate content is quite similar (around 20 %).

Colour variation measurements have been carried out on the bare and the treated mortars after the field exposure tests and also after accelerated ageing tests under UV irradiation in order to evaluate the stability of the applied coatings. No significant variations in the colour of the mortars are appreciable ($\Delta E^* < 5$) under both UV light and ambient exposure for both the commercial resins applied (Table 7). Moreover, the coatings remain stable, and the high surface hydrophobicity is also maintained as demonstrated by $\Delta\theta$ values (Table 7). On the basis of the present results, the Alpha®SI30 resin is less stable (higher values of both $\Delta\theta$ and ΔE^* after UV ageing and ambient exposure) with respect to the Silres®BS16 one, confirming the trend of sulphate and nitrate decreasing, observed in Fig. 8.

Conclusions

In the present work, two artificial stones, an air hardening calcic lime mortar (ALM) and a natural hydraulic lime mortar (HLM), were used. These two materials were characterized by different mineralogical compositions, petrographic textures, and porosity features.

Alpha®SI30 and Silres®BS16 resins were applied to the bare mortars to give hydrophobic features; both Si-based polymers may be used as protective agents for stone materials since high surface hydrophobicity ($\theta > 100^\circ$), scarce water capillary absorption and excellent vapour transpirability were achieved. Comparing the two polymers, Alpha®SI30, notwithstanding the higher features in hydrophobicity, transpirability and capillarity, seems to have lower chemical stability after UV ageing and ambient exposure (higher ΔE^* values and appreciable contact angle lowering) with respect to the Silres®BS16 one.

Further, the final performances of the coatings in terms of reduction of salts formation (i.e. sulphate and nitrate formation) after a prolonged exposure to a polluted environment (two different sites in the present case, i.e. Unimi campus and Milan city centre) were studied. Both the hydrophobizing compounds lead to a nitrate decrease, while in the case of ALM, the lowering in sulphate content is not achieved by both polymers, probably due to the presence of portlandite phase. The combined effect of these factors indicates that Silres®BS16 seems to be promising as protective coating agent in the field of historical building reconstruction.

It is worth noting that besides the necessary laboratory testing, the exposure to real environments is strictly mandatory; unfortunately, these tests underline that a partial deterioration of the coatings occurs in all the treated mortars.

Table 7 Static contact angles ($\Delta\theta$) and colorimetric (ΔE^*) variations after UV (40 h) and ambient (110 days) exposures for coated mortars

Sample	After UV exposure (40 h)		After ambient exposure (110 days)	
	$\Delta\theta/^\circ$	ΔE^*	$\Delta\theta/^\circ$	ΔE^*
HLM_SI30	-26	1.7	-30	3.4
HLM_BS16	-9	2.9	-18	2.1
ALM_SI30	-21	1.5	-25	5.2
ALM_BS16	-2	2.9	-14	2.0

References

- Alessandrini G, Aglietto M, Castelvetro V, Ciardelli F, Peruzzi R, Toniolo L (2000) Comparative evaluation of fluorinated and unfluorinated acrylic copolymers as water-repellent coating materials for stone. *J Appl Polym Sci* 76:962–977. doi:10.1002/(SICI)1097-4628(20000509)76:6<962::AID-APP24>3.0.CO;2-Z
- Belfiore CM, Barca D, Bonazza A, Comite V, la Russa MF, Pezzino A, Ruffolo SA, Sabbioni C (2013) Application of spectrometric analysis to the identification of pollution sources causing cultural heritage damage. *Environ Sci Pollut Res* 20:8848–8859. doi:10.1007/s11356-013-1810-y
- Belfiore CM, Fichera GV, La Russa MF, Pezzino A, Ruffolo SA, Galli G, Barca D (2015) A multidisciplinary approach for the archaeometric study of pozzolanic aggregate in Roman mortars: the case of Villa dei Quintili (Rome, Italy). *Archaeometry* 57:269–296. doi:10.1111/arc.12085
- Brandon CJ, Hohlfelder RL, Jackson MD, Oleson JP (2014) Building for eternity: the history and technology of Roman concrete engineering in the sea. J.P. Oleson, Oxbow Books, Oxford
- Brimblecombe P (2003) The effects of air pollution on the built environment. Imperial College Press, London
- Cappelletti G, Ardizzone S, Meroni D, Soliveri G, Ceotto M, Biaggi C, Benaglia M, Raimondi L (2013) Wettability of bare and fluorinated silanes: a combined approach based on surface free energy evaluations and dipole moment calculations. *J Colloid Interface Sci* 389:284–291. doi:10.1016/j.jcis.2012.09.008
- Cappelletti G, Fermo P, Camilioni M (2015) Smart hybrid coatings for natural stones conservation. *Prog Org Coat* 78:511–516. doi:10.1016/j.porgcoat.2014.05.029
- Carobbi G (1971) Trattato di Mineralogia. Vol. 2, 3rd ed., USES, Firenze
- Doehne E, Price CA (2010) Stone conservation: an overview of current research, 2nd edition. Book. doi: 10.1016/0006-3207(70)90031-5
- Elsen J (2006) Microscopy of historic mortars—a review. *Cem Concr Res* 36:1416–1424. doi:10.1016/j.cemconres.2005.12.006
- Faria P, Henriques F, Rato V (2008) Comparative evaluation of lime mortars for architectural conservation. *J Cult Herit* 9:338–346. doi:10.1016/j.culher.2008.03.003
- Fermo P, Cappelletti G, Cozzi N, Padeletti G, Kaciulis S, Brucalè M, Merlini M (2014a) Hydrophobizing coatings for cultural heritage. A detailed study of resin/stone surface interaction. *Appl Phys A Mater Sci Process* 116:341–348. doi:10.1007/s00339-013-8127-z
- Fermo P, Turrión RG, Rosa M, Omegna A (2014b) A new approach to assess the chemical composition of powder deposits damaging the stone surfaces of historical monuments. *Environ Sci Pollut Res*. doi:10.1007/s11356-014-3855-y
- Fratini F, Pecchioni E, Cantisani E (2008) The petrographic study in the ancient mortars characterization. Dissertation, Historical Mortars Conference, Characterization, Diagnosis, Conservation, Repair and Compatibility, HMC08 Lisboa
- Ghedini N, Ozga I, Bonazza A, Dilillo M, Cachier H, Sabbioni C (2011) Atmospheric aerosol monitoring as a strategy for the preventive conservation of urban monumental heritage: The Florence Baptistery. *Atmos Environ* 45:5979–5987. doi:10.1016/j.atmosenv.2011.08.001
- Gulotta D, Bertoldi M, Bortolotto S, Fermo P, Piazzalunga A, Toniolo L (2013) The Angera stone: a challenging conservation issue in the polluted environment of Milan (Italy). *Environ Earth Sci* 69:1085–1094. doi:10.1007/s12665-012-2165-2
- Jackson M, Marra F (2006) Roman stone masonry: volcanic foundations of the ancient city. *Am J Archaeol* 110:403–436. doi:10.3764/aja.110.3.403
- Kaelble DH (1970) Dispersion-polar surface tension properties of organic solids. *J Adhes* 2:66–81. doi:10.1080/0021846708544582
- Kapridaki C, Marvelaki-Kalaitzaki P (2013) TiO₂-SiO₂-PDMS nanocomposite hydrophobic coating with self-cleaning properties for marble protection. *Prog Org Coat* 76:400–410. doi:10.1016/j.porgcoat.2012.10.006
- Karatasios I, Theoulakis P, Kalagri A, Sapalidis A, Kilikoglou V (2009) Evaluation of consolidation treatments of marly limestones used in archaeological monuments. *Constr Build Mater* 23:2803–2812. doi:10.1016/j.conbuildmat.2009.03.001
- La Russa MF, Ruffolo SA, Rovella N, Belfiore CM, Palermo AM, Guzzi MT, Crisci GM (2012) Multifunctional TiO₂ coatings for cultural heritage. *Prog Org Coat* 74:186–191. doi:10.1016/j.porgcoat.2011.12.008
- La Russa MF, Belfiore CM, Comite V, Barca D, Bonazza A, Ruffolo SA, Crisci GM, Pezzino A (2013) Geochemical study of black crusts as a diagnostic tool in cultural heritage. *Appl Phys A* 113:1151–1162. doi:10.1007/s00339-013-7912-z
- Mahy M, Van Eycken L, Oosterlinck A (1994) Evaluation of uniform color spaces developed after the adoption of CIELAB and CIELUV. *Color Res Appl* 19:105–121. doi:10.1111/j.1520-6378.1994.tb00070.x
- Manoudis PN, Karapanagiotis I, Tsakalof A, Zuburtikudis I, Kolinkeová B, Panayiotou C (2009a) Superhydrophobic films for the protection of outdoor cultural heritage assets. *Appl Phys A Mater Sci Process* 97:351–360. doi:10.1007/s00339-009-5233-z
- Manoudis PN, Tsakalof A, Karapanagiotis I, Zuburtikudis I, Panayiotou C (2009b) Fabrication of super-hydrophobic surfaces for enhanced stone protection. *Surf Coat Technol* 203:1322–1328. doi:10.1016/j.surfcoat.2008.10.041
- Moropoulou A, Bakolas A, Bisbikou K (2000) Investigation of the technology of historic mortars. *J Cult Herit* 1:45–58. doi:10.1016/S1296-2074(99)00118-1
- NORMA UNI 10859 (2000) Cultural Heritage - Natural and Artificial Stones - Determination of water absorption by capillarity
- Owens DK, Wendt R (1969) Estimation of the surface free energy of polymers. *J Appl Polym Sci* 13:1741–1747. doi:10.1592/phco.30.10.1004
- Pecchioni E, Malesani P, Bellucci B, Fratini F (2005) Artificial stones utilised in Florence historical palaces between the XIX and XX centuries. *J Cult Herit* 6:227–233. doi:10.1016/j.culher.2005.06.001
- Pecchioni E, Fratini F, Cantisani E (2006) The ancient mortars, an attestation of the material culture: the case of Florence. *Period Mineral* 75:255–262
- Pecchioni E, Fratini F, Cantisani E (2008) Le malte antiche e moderne tra tradizione e innovazione. Ed. Pàtron Bologna
- Pecchioni E, Fratini F, Cantisani E (2014) Atlas of the ancient mortars in thin section under optical microscope. Nardini Editore, Firenze, p 78
- Rodrigues JD, Grossi A (2007) Indicators and ratings for the compatibility assessment of conservation actions. *J Cult Herit* 8:32–43. doi:10.1016/j.culher.2006.04.007
- Ruffolo SA, La Russa MF, Aloise P, Belfiore CM, Macchia A, Pezzino A, Crisci GM (2014) Efficacy of nanolime in restoration procedures of salt weathered limestone rock. *Appl Phys A Mater Sci Process* 114:753–758. doi:10.1007/s00339-013-7982-y
- Ruffolo SA, Comite V, La Russa MF, Belfiore CM, Barca D, Bonazza A, Crisci GM, Pezzino A, Sabbioni C (2015) An analysis of the black crusts from the Seville Cathedral: a challenge to deepen the understanding of the relationships among microstructure, microchemical features and pollution sources. *Sci Total Environ* 502:157–166. doi:10.1016/j.scitotenv.2014.09.023
- Tidblad J, Kucera V, Ferm M, Kreislova K, Brüggerhoff S, Doytchinov S, Srepani A, Grøntoft T, Yates T, De La Fuente D, Roots O, Lombardo T, Simon S, Faller M, Kwiatkowski L, Kobus J, Vartosos C, Tzanis C, Krage L, Schreiner M, Melcher M, Grancharov I, Karmanova N (2012) Effects of air pollution on materials and cultural heritage: ICP materials celebrates 25 years of research. *Int J Corros* 2012:Article ID 496321, 16 pages. doi: 10.1155/2012/496321

- Tsakalof A, Manoudis P, Karapanagiotis I, Chrysoulakis I, Panayiotou C (2007) Assessment of synthetic polymeric coatings for the protection and preservation of stone monuments. *J Cult Herit* 8:69–72. doi:[10.1016/j.culher.2006.06.007](https://doi.org/10.1016/j.culher.2006.06.007)
- UNI EN 1936 (2001) Determination of apparent density and total open porosity
- UNI EN 15803 (2009) Conservation of cultural property - Test methods - Determination of water vapour permeability
- UNI EN 459-1 (2010) Calci da costruzione - Parte 1: Definizioni, specifiche e criteri di conformità. Ed. UNI (Ente Nazionale Italiano Unificazione) Milano
- Watt J, Tidblad J, Kucera V, Hamilton R (2009) The effects of air pollution on cultural heritage. Springer, New York
- Young T (1805) An essey on cohesion of fluids. *Philos Trans R Soc London* 95:65–87
- Zappia G, Sabbioni C, Riontino C, Gobbi G, Favoni O (1998) Exposure tests of building materials in urban atmosphere. *Sci Total Environ* 224:235–244. doi:[10.1016/S0048-9697\(98\)00359-3](https://doi.org/10.1016/S0048-9697(98)00359-3)
- Zielecka M, Bujnowska E (2006) Silicone-containing polymer matrices as protective coatings. *Prog Org Coat* 55:160–167. doi:[10.1016/j.porgcoat.2005.09.012](https://doi.org/10.1016/j.porgcoat.2005.09.012)